EUROFUSION WPPFC-PR(16) 14723

S Ratynskaia et al.

Tungsten dust remobilization under steady-state and transient plasma conditions

Preprint of Paper to be submitted for publication in
22nd International Conference on Plasma Surface Interactions
in Controlled Fusion Devices (22nd PSI)

This work has been carried out within the framework of the EUROfusion Consortium and has received funding from the Euratom research and training programme 2014-2018 under grant agreement No 633053. The views and opinions expressed herein do not necessarily reflect those of the European Commission.

Tungsten dust remobilization under steady-state and transient plasma conditions

S. Ratynskaia,[1] P. Tolias,[1] M. De Angeli,[2] V. Weinzettl,[3] J. Matejicek,[3] I. Bykov,[4] D. L. Rudakov,[4] L. Vignitchouk,[1] E. Thorén,[1] G. Riva,[5] D. Ripamonti,[5] T. Morgan,[6] R. Panek,[3] G. De Temmerman[7]

[1] *Space and Plasma Physics - KTH Royal Institute of Technology, Teknikringen 31, 10044 Stockholm, Sweden*
[2] *Istituto di Fisica del Plasma - Consiglio Nazionale delle Ricerche, via Cozzi 53, 20125 Milan, Italy*
[3] *Institute of Plasma Physics, Czech Academy of Sciences, Prague, Czech Republic*
[4] *University of California, San Diego, La Jolla, CA 92093-0417, USA*
[5] *Institute of Condensed Matter Chemistry and Energy Technologies - Consiglio Nazionale delle Ricerche, via Cozzi 53, 20125 Milan, Italy*
[6] *FOM Institute DIFFER, Dutch Institute For Fundamental Energy Research, Eindhoven, The Netherlands*
[7] *ITER Organization, Route de Vinon-sur-Verdon, CS 90 046, 13067 St. Paul Lez Durance Cedex, France*

Abstract

Remobilization is one of the most prominent unresolved fusion dust-relevant issues, strongly related to the lifetime of dust in plasma-wetted regions, the survivability of dust on hot plasma-facing surfaces and the formation of dust accumulation sites. A systematic cross-machine study has been initiated to investigate the remobilization of tungsten micron-size dust from tungsten surfaces implementing a newly developed technique based on controlled pre-adhesion by gas dynamics methods. It has been utilized in a number of devices and has provided new insights on remobilization under steady-state and transient conditions. The experiments are interpreted with contact mechanics theory and heat conduction models.

1. Introduction

Dust is the collective term used for condensed particulates (solid, liquid) of sizes ranging from a few nanometers to hundreds of micrometers. It poses a safety problem for future fusion devices such as ITER, since during the nuclear phases of operation it will be tritiated, chemically reactive and toxic [1, 2]. The first dedicated survey in JET with the ITER-Like-Wall detected tungsten and beryllium dust with diameters up to $\sim 5\,\mu$m [3]. Systematic collection activities in the full-W ASDEX-Upgrade revealed most probable diameters $< 1-2\,\mu$m and sizes up to $53\,\mu$m [4].

Be and even W dust embedded in dense ITER-like edge plasmas will promptly vaporize unless it adheres to the cooler plasma-facing components (PFCs). The process of remobilization, *i.e.* the in-plasma release of dust stuck at vessel locations away from its production site, is an integral part of the physics of dust in fusion devices which stands on an equal footing with the process of transport. Dust transport has been extensively studied during the last decade by dust dynamics codes [5, 6, 7] which have been employed for the modelling of dedicated dust injection experiments and intrinsic dust trajectories [8, 9, 10, 11, 12, 13, 14]. On the other hand, dust remobilization has only been recently studied [15, 16] in spite of the fact that the interaction of adhered metallic dust with steady-state and transient plasmas is central to diverse plasma-wall interaction issues: (i) the lifetime of dust in plasma-wetted regions of the vessel which is correlated with dust inventories and recycling, (ii) the survivability of dust on hot plasma-facing surfaces which is connected with safety issues, (iii) the formation of dust accumulation sites which need to be targeted for monitoring and removal, (iv) the specification of realistic initial and terminal conditions for dust trajectories which constitutes an important input for dust dynamics codes.

Here, we shall summarize the main results and lessons learnt from systematic cross-machine studies of W dust remobilization from planar W surfaces [15, 16]. Spherical W dust is employed with $5-25\,\mu$m diameter. The experiments implement a newly developed technique based on controlled pre-adhesion by gas dynamics methods that mimics sticking as it naturally occurs in tokamaks. It has been utilized in a number of devices (DIII-D, Pilot-PSI, TEXTOR, COMPASS, EXTRAP-T2R) and has provided an abundance of data on remobilization under steady-state and transient conditions. We shall also discuss the current status of modelling efforts that are based on contact mechanics theory [15] and heat conduction simulations [16].

2. Remobilization under steady-state conditions

2.1. Experimental results

Systematic W-on-W remobilization experiments [15] were carried out in the Pilot-PSI linear device [17] and complemented with experiments in the TEXTOR limiter tokamak (with Mo, Ti dust as W proxies) and the reversed-field pinch EXTRAP-T2R. Planar samples with pre-adhered dust were exposed under varying B-field topologies and plasma conditions: $n = 10^{17} - 6\times10^{20}\,\mathrm{m}^{-3}$, $T_\mathrm{e} = 0.4-15\,\mathrm{eV}$, $T_\mathrm{i} = 0.4-10\,\mathrm{eV}$, $\lambda_\mathrm{D}/R_\mathrm{d} = 10^{-2}-10$, $\measuredangle \boldsymbol{B} = 5^\circ-90^\circ$. See Fig.1 for an example. It was established that larger dust and agglomerates remobilize much easier than smaller grains $\lesssim 10\,\mu$m. The remobilization activity, the ratio of

the detached over the overall pre-adhered dust number, was an increasing function of the size. This implies that smaller dust can be expected to reside longer on PFCs, but also that size distributions inferred from post-mortem dust collection activities do not directly reflect the *in situ* distributions created by various generation mechanisms.

In Pilot-PSI, it was discerned that sample re-exposure under identical conditions does not lead to any additional remobilization, suggesting the existence of remobilization conditions and the absence of hysteresis effects (no strong contact modification due to heat absorption or hydrogen adsorption). Cameras were employed to distinguish which remobilization condition is realized, results were inconclusive since dust was always observed after the detachment instant; either vision was obscured by cumulative thermal radiation from the whole adhered dust population or dust was initially not incandescent enough [15, 18].

2.2. Theoretical results

Remobilization occurs when plasma-induced forces overcome the contact forces (adhesion and static friction). In steady-state plasmas, the dust temperature is far from the W melting point, thus, the contact, as quantified by the contact radius a and the depth of indentation δ, is not altered by energy exchange with the plasma. We denote the plasma-induced force with a line of action traversing the dust center of mass by $\boldsymbol{F}_{\rm pl}$, the plasma-induced moment of surface stresses about the center by $\boldsymbol{M}_{\rm pl}$, the minimum normal force necessary to overcome adhesion or pull-off force by $\boldsymbol{F}_{\rm po}$, the static friction coefficient by $\mu_{\rm s}$. Generic remobilization conditions can be found by force balance in the normal / tangential directions as well as torque balance around the contact point [15, 19, 20] (see Fig.2 insert):

$$\begin{aligned} &\underline{\textit{direct lift-up}}: F_{\rm pl}^{\rm n} > F_{\rm po}\,, \\ &\underline{\textit{sliding}}: F_{\rm pl}^{\rm t} > \mu_{\rm s}\left(F_{\rm po} - F_{\rm pl}^{\rm n}\right)\,, \\ &\underline{\textit{rolling}}: M_{\rm pl} + F_{\rm pl}^{\rm t}(R_{\rm d} - \delta) > \left(F_{\rm po} - F_{\rm pl}^{\rm n}\right) a\,. \end{aligned} \tag{1}$$

Contact mechanics descriptions but also microscopic theories of adhesion predict that $F_{\rm po} \propto R_{\rm d}$. On the other hand, plasma-induced forces due to particle scattering, particle absorption and interaction with mean electrostatic fields are roughly proportional to the dust surface, scaling as $F_{\rm pl} \propto R_{\rm d}^2$. Inspecting Eqs.(1), the above suggest that larger grains can be easier remobilized by the plasma (see Fig.2). Finally, volume forces such as gravity scale as $F_{\rm g} \propto R_{\rm d}^3$ and are negligible in dust remobilization studies.

Despite the straightforward nature of these conditions, theoretical predictions are challenging owing to: (i) *Uncertainties in the contact forces.* Concerning the pull-off force, the Johnson–Kendall–Roberts theory [21] yields $F_{\rm po}^{\rm JKR} = (3/2)\pi R_{\rm d}\Delta\gamma$, whereas the Derjaguin–Muller–Toporov theory [22] yields $F_{\rm po}^{\rm DMT} = 2\pi R_{\rm d}\Delta\gamma$ with $\Delta\gamma = 2\gamma$ for the work of adhesion, $\gamma = 4.36\,{\rm J/m^2}$ for the W surface energy. Recent measurements [23] revealed that contact mechanics models overestimate W-on-W adhesion by nearly two orders of magnitude, while Van der Waals theory provides values close to the experimental, $F_{\rm po}^{\rm VdW} = [A/(6z_0^2)]R_{\rm d}$ for a distance of closest approach equal to the lattice parameter 3.16 Å and a Hamaker constant $A = 4\times10^{-19}\,{\rm J}$. Concerning the friction force, Amontons's law is not fully established for microscopic bodies [24] and $\mu_{\rm s}$ is hard to quantify. (ii) *Unknown plasma-induced forces.* The well-known expression for the ion drag force is not valid in the sheath [25], whereas the Lebedev expression for the electrostatic contact force is not valid in plasmas [26]. Analytic expressions cannot be derived for sheath-within-a-sheath problems, but particle-in-cell codes can provide quantitative results for $\boldsymbol{F}_{\rm pl}$, $\boldsymbol{M}_{\rm pl}$. (iii) *Probabilistic character of roughness.* Surface roughness leads to statistical variations in the pull-off and friction forces, but can also alter the remobilization conditions [15]. In absence of roughness, the remobilization activity would jump from zero to unity at a threshold radius, which contradicts the experiments.

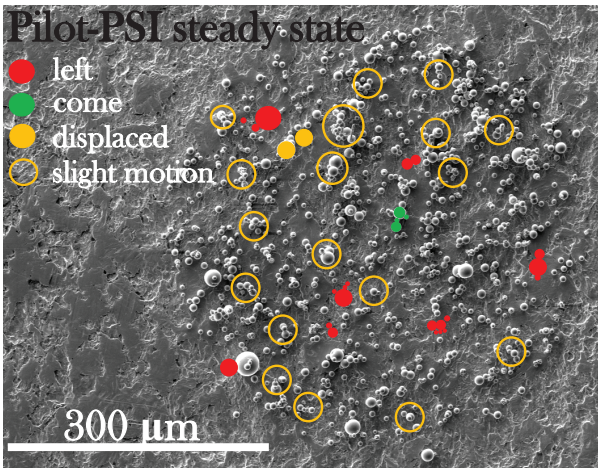

Figure 1: An example of low remobilization activity. Overlaid SEM image of a W-on-W spot prior to and post exposure to the Pilot-PSI steady-state plasma ($B = 0.4\,{\rm T}$, $\measuredangle\boldsymbol{B} = 10°$, $t = 2\,{\rm s}$). Color coding is as follows; dust that was removed from its initial position (red), dust that appeared post exposure (green), dust that was clearly displaced (orange). There are 18 events of slight (of the order of the dust radius) displacements, rotations and cluster re-arrangements. Notice that exposure affected agglomerates and the largest dust, while small isolated grains retained their original position.

3. Remobilization under transient conditions

3.1. Experimental results

Systematic experiments addressing the interaction of adhered W dust with transient ELM-like plasma fluxes [16] were conducted in Pilot-PSI [17, 27] and complemented with experiments in DIII-D. In Pilot-PSI, W-on-W samples were exposed with $\measuredangle\boldsymbol{B} = 10°$ or 90° to single, multiple and repetitive ELM-like pulses of $\Delta\tau = 1\,{\rm ms}$, $q_\perp = 35 - 550\,{\rm MW/m^2}$ with the peak W substrate surface temperature reaching up to 1800° C. In DIII-D, W-on-W samples were exposed flush with $\measuredangle\boldsymbol{B} = 1.1° - 2.5°$ in the lower DIII-D divertor during ELMing H-mode discharges [28] to

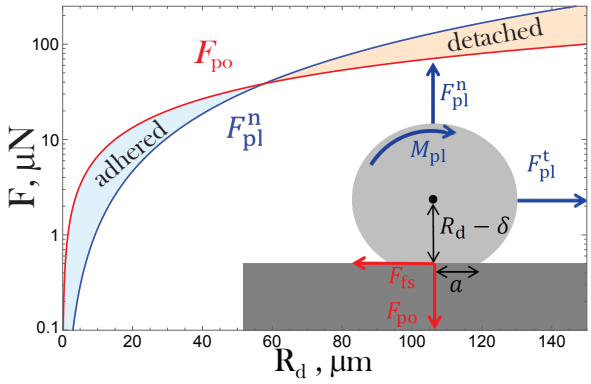

Figure 2: W dust remobilization by direct lift-up for deuterium plasmas relevant for the ITER divertor: $n_\mathrm{i} = 10^{20}\,\mathrm{m}^{-3}$, $T_\mathrm{i} = T_\mathrm{e} = 10\,\mathrm{eV}$, unity ion Mach number and $z = -e\phi_\mathrm{d}/T_\mathrm{e} = 3$ for the normalized dust potential. The pull-off force follows the Van der Waals expression. Heuristically, it is assumed that the plasma-induced forces are represented by the ion drag force [25] and that the average Coulomb logarithm is size-independent with $\langle \ln \Lambda_\mathrm{i} \rangle = 3$. $F^\mathrm{n}_\mathrm{pl} > F_\mathrm{po}$ for large sizes, leading to remobilization. We emphasize that the ion drag force assumption is not valid, it was followed to illustrate how size selectivity stems from the different R_d-scalings. In experiments, mainly due to roughness, there is no sharp size threshold [15]. (Insert) Force diagram for a spherical dust grain adhered to a smooth planar PFC.

hundreds of ELMs of $\Delta\tau = 0.4{-}0.8\,\mathrm{ms}$, $q_\perp = 1{-}5\,\mathrm{MW/m^2}$ with the W substrate surface temperature below 600° C.

In contrast to the steady-state, the behavior of adhered dust was not only affected by momentum exchange but also by energy exchange with the plasma. The contact was altered at elevated dust temperatures and macro-morphological changes occurred when the melting point was exceeded. The main results can be summarized as follows [16], see also Fig.3: **(i)** Melting of W agglomerates was consistently observed, but there were no evidence of isolated dust melting or bulk substrate modification. Dust clusters melted under lower heat loads than bulk materials, the maximum heat flux factor $F_\mathrm{HF} = q_\perp\sqrt{\Delta\tau}$ was $17.4\,\mathrm{MWm^{-2}s^{1/2}}$, much lower than the melting threshold of bulk W [29]. Essentially, the top grains are thermally insulated from the substrate owing to the smallness of the contact area, the imperfection of the thermal contact and the (multiple) mediating grain(s). For oblique exposures, we note that dust is also subject to $q_\parallel$ similar to PFC edges. **(ii)** The novel mechanism of wetting-induced coagulation was observed which transforms small dust clusters into single large grains. Top grains receive most of the incident heat flux, whereas bottom grains are geometrically shadowed and receive less heat flux through conduction. The top grains melt and spread on the bottom solid grains, but due to the short ELM duration resolidification occurs prior to substrate wetting. The interplay between the melting, spreading and re-solidification rates is such that spherical grains rather than planar films are preferentially generated. Frozen capillary waves at the bottom of the newly formed dust are relics of this competition. **(iii)** Despite their larger size, newly formed grains have a low remobilization tendency due to contact strengthening by liquid spreading and solid sintering. For similar reasons, remobilization under transients is not enhanced compared to the steady-state (at least in Pilot-PSI, where experiments for both cases have been conducted).

These cross-machine studies [16] were recently complemented by experiments in COMPASS. W-on-W samples were mounted on the graphite head of a manipulator allowing insertion close to the divertor with $\measuredangle \boldsymbol{B} = 43°$ and exposed during ELMing H-mode discharges [30] to tens of ELMs of $\Delta\tau = 0.2 - 0.3\,\mathrm{ms}$ and $q_\perp \lesssim 1\,\mathrm{MW/m^2}$. The heat flux was not high enough for clusters to melt, hence, in principle, momentum exchange of adhered dust with transients was decoupled from the dominating energy exchange aspects. Enhanced remobilization was observed on confined areas of $\lesssim 100\,\mu\mathrm{m}$ width ($\varnothing = 0.5\,\mathrm{mm}$ for the dust spot), while other areas remained nearly intact. Further analysis is required to explain such localization. The first controlled remobilization experiments under disruptions were also performed with W-on-W samples exposed to ELM-free H-mode and L-mode discharges terminated by vertical displacement events towards the samples. Remobilization activity exceeded 50% in localized spot areas (Fig.4a), agglomerates remobilized much easier (Fig.4b), isolated dust was reorganized into clusters / strings (Fig.4c circles) & cluster rearrangements occurred (Fig.4c arrows).

3.2. Theoretical results

The primary goal is to predict whether clusters or isolated dust will melt under ITER-like transient heat loads and for ITER-like PFC surface temperatures. The details of droplet spreading and wetting are of secondary importance. This simplifies the problem, since three-dimensional finite-element heat transfer simulations will suffice.

In Ref.[16], axisymmetric heat conduction simulations were carried out for dust-substrate systems interacting with transient plasmas. In addition to the incident plasma heat flux, dust was subject to cooling by thermal radiation and thermionic emission. The contact radius a was calculated from theoretical models of adhesive elastic-perfectly plastic impacts [31]. Despite their simplicity, the simulations reflected the experimental trend; clusters melted by much lower transient heat fluxes than isolated grains.

However, heat constriction does not only stem from the smallness of the contact area. Due to the surface roughness, the exact temperature profile changes abruptly near the interface. This can be modelled with the thermal conductance per unit area $h_\mathrm{c} = q/\Delta T$, where ΔT is the interface temperature drop and q the incident heat flux [32]. The *total thermal conductance* can be idealized by two conductances in series [33]: the constriction conductance due to the limited circular contact $2ka$ and the contact conductance due to the presence of roughness $\pi a^2 h_\mathrm{c}$, with $k = 2k_\mathrm{d}k_\mathrm{s}/(k_\mathrm{d} + k_\mathrm{s})$ the effective thermal conductivity,

$$G^{-1} = (2ka)^{-1} + (\pi a^2 h_\mathrm{c})^{-1}\,. \qquad (2)$$

For $h_\mathrm{c} \ll 2k/(\pi a) \Rightarrow G \to 0$, which corresponds to perfect thermal insulation. For $h_\mathrm{c} \gg 2k/(\pi a) \Rightarrow G \to 2ka$, which

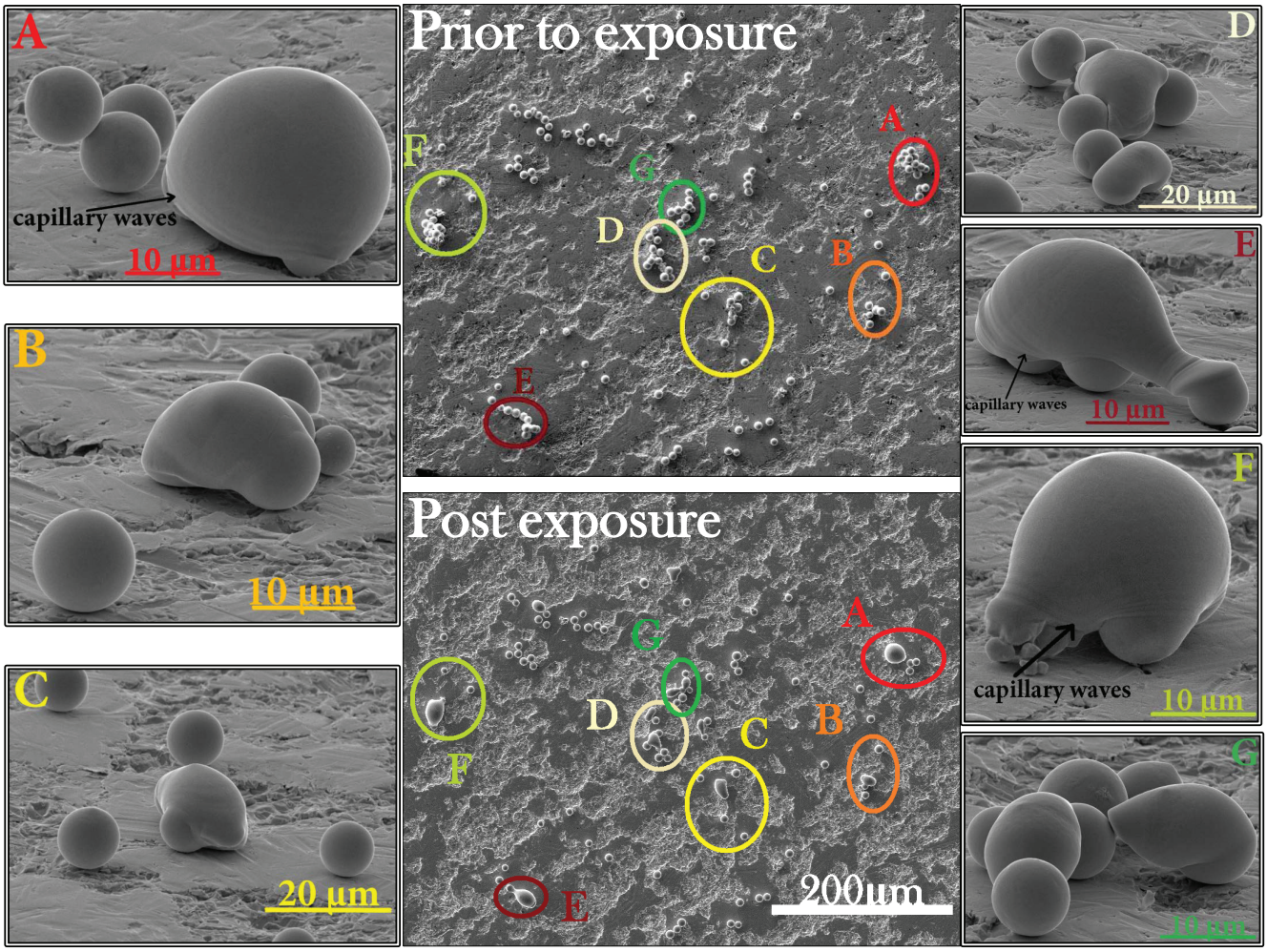

Figure 3: SEM images of a W-on-W spot ($9 \pm 1\,\mu$m diameter dust) before and after three ELM-like Pilot-PSI exposures. 1st, 2nd exposures: $\angle B = 10°$, $B = 1.2\,$T, $\Delta\tau = 1\,$ms, $q_\perp \simeq 35\,$MW/m^2. 3rd exposure: $\angle B = 90°$, $B = 1.6\,$T, $\Delta\tau = 1\,$ms, $q_\perp \simeq 550\,$MW/m^2. (Inserts) Tilted larger magnification SEM images of selected areas of the same spot after exposure: (i) The top grains melted wetting the solid bottom grains, see A-G. (ii) Frozen capillary waves, see A,E,F. (iii) Isolated dust never melted, even close to molten clusters, see B,C,D,G. (iv) Not all clusters melted due to the stochastic nature of the thermal contact, see A,D. (v) Part of some clusters remobilized probably by interacting with the steady-state plasma prior to the ELM-like pulse, compare A to the main figure. This is the only remobilization event in the spot.

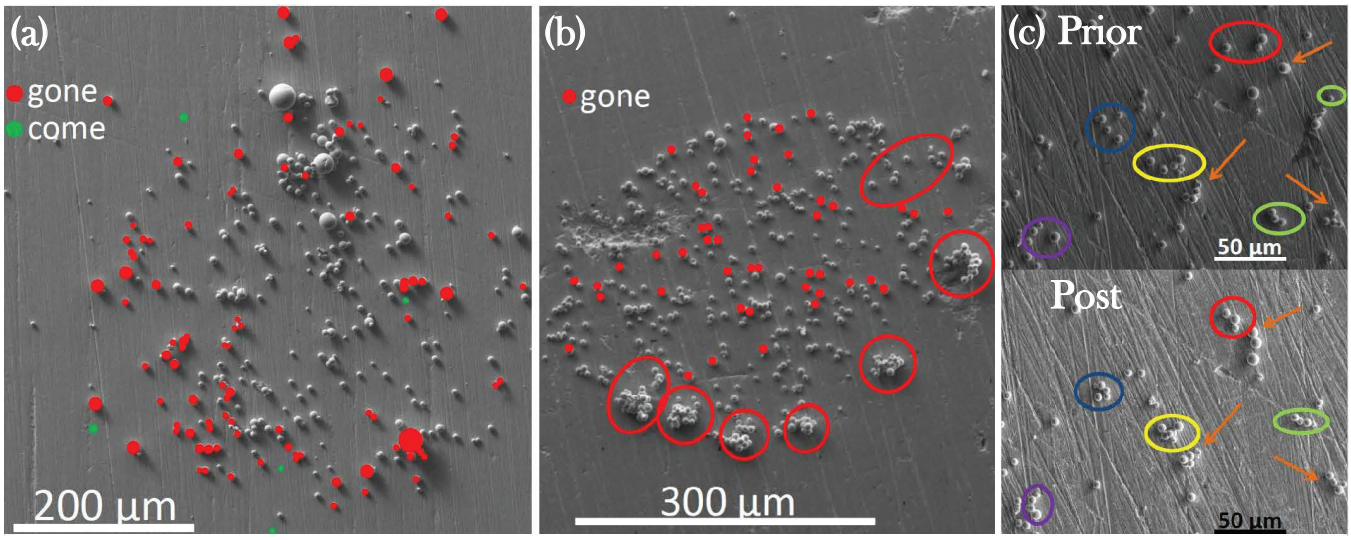

Figure 4: (a,b) Overlaid SEM images of two W-on-W spots prior to and post exposure to COMPASS discharges terminated by VDEs. (c) SEM images of a selected area prior to and post exposure. Circles indicate cluster formation, arrows indicate cluster rearrangement.

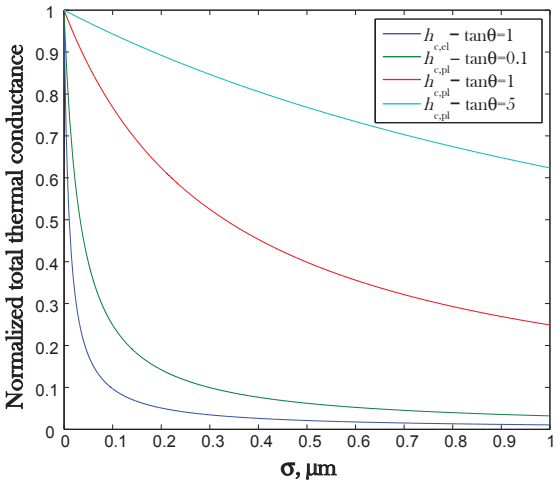

Figure 5: Normalized total thermal conductance $G_{\rm n} = G/2ka$ as a function of the roughness for spherical W dust $R_{\rm d} = 5\,\mu$m adhered to planar W substrates. Regardless of the deformation mode; $\sigma \to 0$ corresponds to perfect thermal contact $G_{\rm n} = 1$, $\sigma \to \infty$ to perfect thermal insulation $G_{\rm n} = 0$. For *elastic deformation*, $h_{\rm c,el}$ is nearly independent of the average slope making a rapid transition between the two asymptotes. Insulation implies that clusters and isolated grains will acquire similar temperatures after interacting with ELMs, contradicting experiments. For *plastic deformation*, $h_{\rm c,pl}$ is proportional to the average slope and exhibits an intermediate behavior.

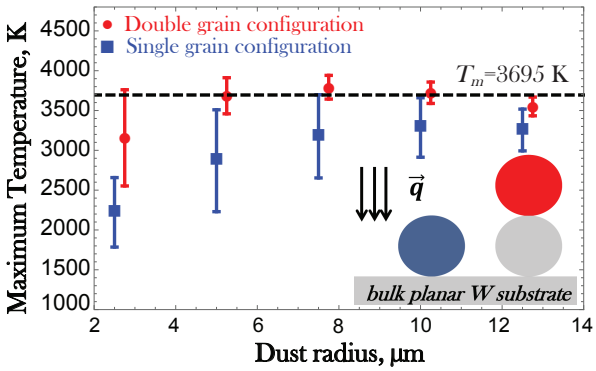

Figure 6: Simulated dust temperature post interaction with a normal square heat flux pulse $q_{\perp} = 200\,{\rm MWm}^{-2}$ of $\Delta\tau = 1\,$ms as a function of the adhered W dust radius. The initial system temperature is uniform with a value 920 K that matches the Pilot-PSI IR camera data. The thermal contact conductance is included after Eq.(4), the upper/lower error bars correspond to $\sigma = 0.2/0.05\,\mu$m and it is assumed that $\tan\theta = 0.1$. In the double grain configuration (see insert), only the temperature of the top grain is shown. The horizontal dashed line refers to the melting point of W. The results confirm that clusters are more susceptible to melting than isolated grains.

corresponds to perfect thermal contact. Many theoretical models exist for the thermal contact conductance per unit area, the exact $h_{\rm c}$ expression mainly depends on the mode of deformation [34]. For *elastic deformation* [35]

$$h_{\rm c,el} \simeq 2.15\left[k(\tan\theta)^{0.06}/\sigma\right](P/E^*)^{0.94}\,, \qquad (3)$$

with P the pressure between the surfaces, $\sigma = \sqrt{\sigma_{\rm d}^2 + \sigma_{\rm s}^2}$ with $\sigma_i \ll a$ the standard deviation of the roughness asperity height, $\tan\theta = \sqrt{\tan^2\theta_{\rm d} + \tan^2\theta_{\rm s}}$ with $\tan\theta_i$ the mean absolute asperity slope. For *plastic deformation* [35, 36]

$$h_{\rm c,pl} \simeq 1.13\left[k\tan\theta/\sigma\right](P/H)^{0.94}\,, \qquad (4)$$

with H the micro-hardness of the softer body in contact.

Due to the onset of plasticity for ITER-relevant sticking impacts [15], $h_{\rm c,pl}$ is more appropriate. Moreover, plots of the normalized total thermal conductance $G/2ka$ versus the effective rms roughness reveal that for elastic deformation dust is essentially insulated, whereas for plastic deformation dust exhibits an intermediate behavior between perfect contact and perfect insulation (see Fig.5). Inclusion of $h_{\rm c,pl}$ to the heat transfer simulations significantly improves agreement with experiments and justifies the observed statistical nature of cluster melting (see Fig.6).

4. Summary and implications

Experiments under steady state plasma conditions confirmed that only large dust and agglomerates can be effectively detached from PFCs and corroborated the crucial role of adhesion in remobilization. Theoretical modelling based on momentum balance between the plasma-induced and the contact forces can explain the observed size dependence. Experiments under transient plasma conditions displayed the importance of energy exchange which inhibits remobilization enhancement during ELMs, revealed that dust clusters can melt under much lower heat loads than bulk materials and documented the strong survivability of dust residing on hot plasma-wetted areas as well as its ability to grow through wetting-induced coagulation. Numerical modelling based on heat transfer simulations considering heat constriction due to the smallness of the contact area and the presence of roughness can reproduce the main experimental trends.

The synergy between experiments and theory has provided confidence that the main physics involved in dust remobilization have been identified. The major obstacles in the efforts towards quantitative modelling are connected to the analytically intractable sheath-within-a-sheath problem (uncertainties in plasma momentum and heat transfer), the omnipresent multi-scale roughness (addition of a probabilistic component to the contact forces and the thermal contact conductance) and the dynamical nature of the contact area at elevated temperatures (augmentation due to macroscopic wetting and microscopic roughness filling).

We have focused on W dust remobilization, due to the large body of experimental and theoretical results available. We point out that DIII-D exposures with Al dust indicate that the phenomena described herein are relevant for metallic dust in general [16]. Future work will focus on: experiments with beryllium proxies since Be is expected to be the main dust constituent in ITER, prolonged exposures under hundreds consecutive ELMs in order to determine whether dust spreading can lead to complete PFC wetting, systematic exposures under disruptions in order

to document their ability to redistribute the dust inventory and analyze their specific remobilization mechanisms [37] (PFC vibrations, large induced currents).

In lieu of concluding remarks, we shall pose an open question: *Is it preferable for fusion reactors that dust is easily remobilizable or that dust is strongly adhered?* Dust remobilizing in edge plasmas will be a localized source of impurities, whereas dust remobilizing upon loss-of-vacuum accidents will pose a safety issue [38]. On the other hand, strongly adhered dust can compromise PFC integrity, accumulate during operation and will be hard to remove by conventional cleaning methods. Moreover, dust surviving at hot surfaces will pose a safety issue upon loss-of-coolant accidents [39]. The current experimental results indicate that W dust will be strongly adhered, but there is a strong dependence on the size distribution. Reliable extrapolations to ITER require further advances in the theoretical modelling of remobilization but also coupling with the predictions of droplet and dust production codes [40, 41].

Acknowledgments

This work is supported in part by the US DOE under DE-FG02-07ER54917 and DE-FC02-04ER54698. It has been carried out within the framework of the EUROfusion Consortium and has received funding from the Euratom research and training programme 2014-2018 under grant agreement No 633053. Work performed under EUROfusion WP PFC. The views and opinions expressed herein do not necessarily reflect those of the European Commission.

[1] J. Roth, E. Tsitrone, A. Loarte, Th. Loarer *et al.*, *J. Nucl. Mater.* **390** (2009) 1.
[2] M. Shimada, R. A. Pitts, S. Ciattaglia, S. Carpentier *et al.*, *J. Nucl. Mater.* **438** (2013) S996.
[3] A. Baron-Wiechec, E. Fortuna-Zaleśna, J. Grzonka, M. Rubel *et al.*, *Nucl. Fusion* **55** (2015) 113033.
[4] M. Balden, N. Endstrasser, P. W. Humrickhouse, V. Rohde *et al.*, *Nucl. Fusion* **54** (2014) 073010.
[5] S. I. Krasheninnikov, R. D. Smirnov and D. L. Rudakov, *Plasma Phys. Control. Fusion* **53** (2011) 083001.
[6] L. Vignitchouk, P. Tolias and S. Ratynskaia, *Plasma Phys. Control. Fusion* **56** (2014) 095005.
[7] M. Bacharis, M. Coppins and J. E. Allen, *Phys. Plasmas* **17** (2010) 042505.
[8] D. L. Rudakov, A. Litnovsky, W. P. West, J. H. Yu *et al.*, *Nucl. Fusion* **49** (2009) 085022.
[9] G. De Temmerman, M. Bacharis, J. Dowling and S. Lisgo, *Nucl. Fusion* **50** (2010) 105012.
[10] R. D. Smirnov, S. I. Krasheninnikov, A. Yu. Pigarov, A. L. Roquemore *et al.*, *J. Nucl. Mater.* **415** (2011) S1067.
[11] S. Ratynskaia, C. Castaldo, H. Bergsåker and D. Rudakov, *Plasma Phys. Control. Fusion* **53** (2011) 074009.
[12] S. Ratynskaia, L. Vignitchouk, P. Tolias, I. Bykov *et al.*, *Nucl. Fusion* **53** (2013) 123002.
[13] J. C. Flanagan, M. Sertoli, M. Bacharis, G. F. Matthews *et al.*, *Plasma Phys. Control. Fusion* **57** (2015) 014037.
[14] A. Shalpegin, L. Vignitchouk, I. Erofeev, F. Brochard *et al.*, *Plasma Phys. Control. Fusion* **57** (2015) 125017.
[15] P. Tolias, S. Ratynskaia, M. De Angeli, G. De Temmerman *et al.*, *Plasma Phys. Control. Fusion* **58** (2016) 025009.
[16] S. Ratynskaia, P. Tolias, I. Bykov, D. Rudakov *et al.*, *Nucl. Fusion* **56** (2016) 066010.
[17] G. De Temmerman, J. J. Zielinski, S. van Diepen, L. Marot and M. Price, *Nucl. Fusion* **51** (2011) 073008.
[18] A. Shalpegin, F. Brochard, S. Ratynskaia, P. Tolias *et al.*, *Nucl. Fusion* **55** (2015) 112001.
[19] M. A. Hubbe, *Colloids Surf.* **12** (1984) 151
[20] G. M. Burdick, N. S. Berman and S. P. Beaudoin, *J. Nanopart. Res.* **3** (2001) 455.
[21] K. L. Johnson, K. Kendall and A. D. Roberts, *Proc. R. Soc. A* **324** (1971) 301.
[22] B. Derjaguin, V. M. Muller and Y. P. Toporov, *J. Colloid Interface Sci.* **53** (1975) 314.
[23] G. Riva, P. Tolias, *et al.*, "Adhesion measurements for tungsten dust deposited on tungsten surfaces", these proceedings
[24] M. H. Müser, L. Wenning and M. O. Robbins, *Phys. Rev. Lett.* **86** (2001) 1295.
[25] I. Hutchinson, *Plasma Phys. Control. Fusion* **48** (2006) 185.
[26] N. N. Lebedev and I. P. Skalskaya, *Sov. Phys. Tech. Phys.* **7** (1962) 268.
[27] T. W. Morgan, T. M. de Kruif, H. J. van der Meiden *et al.*, *Plasma Phys. Control. Fusion* **56** (2014) 095004.
[28] C. P. C. Wong, R. Junge, R. D. Phelps *et al.*, *J. Nucl. Mater.* **196198** (1992) 871.
[29] G. Pintsuk, W. Kühnlein, J. Linke and M. Rödig, *Fusion Eng. Des.* **82** (2007) 1720.
[30] R. Panek, J. Adamek, M. Aftanas, P. Bilkova *et al.*, *Plasma Phys. Control. Fusion* **58** (2016) 014015.
[31] C. Thornton and Z. Ning, *Powder Technol.* **99** (1998) 154.
[32] C. V. Madhusudana, *Thermal Contact Conductance*, Springer, Heidelberg, 2014.
[33] M. M. Yovanovich, *Int. J. Heat Mass Transfer* **12** (1969) 1517.
[34] M. M. Yovanovich, *IEEE Trans. Comp. Packag. Technol.* **28** (2005) 182.
[35] B. B. Mikic, *Int. J. Heat Mass Transfer* **17** (1974) 205.
[36] M. G. Cooper, B. B. Mikic and M. M. Yovanovich, *Int. J. Heat Mass Transfer* **12** (1969) 279.
[37] Y. V. Martynenko and M. Y. Nagel, *Plasma Phys. Rep.* **38** (2012) 290.
[38] F. Gensdarmes, C. Grisolia, A. Roynette, S. Peillon *et al.*, *Fusion Eng. Des.* **88** (2013) 2684.
[39] J. P. Sharpe, D. A. Petti and H.-W. Bartels, *Fusion Eng. Des.* **6364** (2002) 153.
[40] J. W. Coenen, B. Bazylev, S. Brezinsek, V. Philipps *et al.*, *J. Nucl. Mater.* **415** (2011) S78.
[41] S. Pestchanyi, I. Garkusha, V. Makhlaj and I. Landman, *Phys. Scr.* **T145** (2011) 014062.